DALTON
FULL PAPER

EPR and UV/VIS spectroscopic investigations of VO^{2+} complexes and compounds formed in alkali pyrosulfates

Søren B. Rasmussen, K. Michael Eriksen and Rasmus Fehrmann *

Department of Chemistry and ICAT (Interdisciplinary Research Center for Catalysis), Technical University of Denmark, DK-2800 Lyngby, Denmark

Received 20th April 2001, Accepted 10th October 2001
First published as an Advance Article on the web 6th December 2001

The catalytically important molten salt–gas system $M_2S_2O_7$–M_2SO_4–V_2O_5/SO_2(g) (M = Na, K, Rb, Cs) has been investigated by X- and Q-band EPR spectroscopy. In order to obtain information about the V(IV) complex formation in the melts, samples rather dilute in V_2O_5 were quenched from the molten state at 450–460 °C to 0 °C. EPR spectra of the quenched samples were recorded on samples with alkali to vanadium (M/V) ratios 40, 80 and 160. The spectra show that two V(IV) complexes dominate in the melt regardless of the type of alkali metal ion. In systems with low activity of sulfate a paramagnetic V(IV) complex with $g_{\|} = 1.915$, $g_{\perp} = 1.978$ and line widths 5–15 Gauss is observed. In systems saturated with M_2SO_4 the obtained EPR spectra show a paramagnetic complex with the *g*-tensors $g_{\|} = 1.930$, $g_{\perp} = 1.980$ and line widths 20–60 Gauss. These results fit very well with the assumption that the species $VO(SO_4)_2^{2-}$ and SO_4^{2-} are in equilibrium with $VO(SO_4)_3^{4-}$. It has also been shown for the system $M_2S_2O_7$–M_2SO_4(sat)–V_2O_5/SO_2(g) that the line widths in the system increase with higher cation radius, and depend linearly on the volume fraction of the sample occupied by the cation. This indicates that spin–spin relaxation effects are the major contribution to line broadening. Combining information from UV/VIS and EPR spectra shows that the VO^{2+} unit in the molten salt solvent exhibits electronic properties close to aqueous solutions of V(IV).

Introduction

The molten salt–gas system $M_2S_2O_7$/M_2SO_4/V_2O_5–SO_2/O_2/SO_3/N_2 (M = Na, K and/or Cs) is generally accepted as a realistic model system of the sulfuric acid catalyst.[1] Earlier work[2] has shown that during catalyst working conditions, an equilibrium between V(IV) and V(V) is found in the catalyst dependent on the SO_2/SO_3 partial pressure ratio. Not much is generally known about the structure of vanadium complexes in pyrosulfate melts. However, recent multi-nuclear NMR investigations[3,4] have shown that V(V) is present as slightly distorted octahedral complexes in the catalytically important concentration range (molar ratio M/V = 2–4). Particularly important has been the X-ray investigation[5] of the compound $Cs_4(VO)_2O(SO_4)_4$ and the subsequent confirmation by NMR spectroscopy that the $(VO)_2O(SO_4)_4^{4-}$ complex exists in the molten state as well as in the solid. A recent Raman spectroscopic investigation[6] on these systems is in accordance with these results. The dimeric anion $(VO)_2O(SO_4)_4^{4-}$ is believed to be the catalytically active component in the catalyst.[7]

The paramagnetic ([Ar]3d^1) vanadyl complex has been thoroughly investigated by EPR for years, however almost entirely in apolar organic solvents or water. The EPR spectra of most vanadyl complexes can be described by a spin Hamiltonian, $\boldsymbol{H}$, including the electron-Zeeman interaction and the electron-vanadium nuclear hyperfine interaction (1):

$$\boldsymbol{H} = \beta H(g_{xx}\hat{S}_x + g_{yy}\hat{S}_y + g_{zz}\hat{S}_z) + hc(A_{xx}\hat{S}_x\hat{I}_x + A_{yy}\hat{S}_y\hat{I}_y + A_{zz}\hat{S}_z\hat{I}_z) \quad (1)$$

where *x*, *y* and *z* is the axis system which diagonalizes both the *g* and nuclear hyperfine *A* tensors. *A* is here expressed in cm^{-1}. β, *h*, *c* and *H* are the Bohr magneton, Planck's constant, the speed of light and the applied magnetic field, respectively. $\hat{S}_i$ and $\hat{I}_i$ ($i = x, y, z$) are the electron and nuclear spin operators. Often X-band spectra can be described by axially symmetric tensors, in which case $g_{\|} = g_{zz}$, $g_{\perp} = g_{xx} = g_{yy}$. For many complexes with symmetry lower than C_{4v} in-plane magnetic anisotropy becomes more evident for Q-band spectra. On the vanadyl cation in molten pyrosulfate, very little is known. Early *in-situ* EPR work[8] indicated two types of V(IV) species present in the catalysts–monomeric and dimeric/polymeric VO^{2+} complexes. Later EPR work has confirmed[9,10] and extended[2] this by showing exclusively monomeric V(IV) complexes at vanadium concentrations far below the catalytically relevant concentration range. Spectroscopic and potentiometric investigations[2,11] have confirmed the existence of an equilibrium between dimeric V(V) and monomeric V(IV) at low vanadium concentrations.

This paper presents the results of an EPR investigation on V(IV) complexes in $M_2S_2O_7$–M_2SO_4–V_2O_5/SO_2(g) (M = Na, K, Rb or Cs) melts at low vanadium concentrations and on precipitating V(IV) compounds at higher concentrations. Melts with low vanadium concentrations allow recording of well resolved EPR spectra on both molten and quenched samples leading to more detailed information on the nature of the complexes, whereas melts with higher concentrations allow the formation of sufficient amounts of crystals to record their powder EPR spectra.

Experimental

Chemicals

Alkali pyrosulfate was made by thermal decomposition of the corresponding peroxodisulfate (analytical grade) as earlier described.[12] $Cs_2S_2O_8$ and $Rb_2S_2O_8$ are not commercially available and were synthesized as described for $Cs_2S_2O_8$.[13] It proved necessary to recrystallize $Na_2S_2O_8$ before decomposition to obtain sufficient purity (>99.9%). V_2O_5 was from Cerac (Pure >99.9%) and used without any further treatment. SO_2 was from AGA (>99.9%). All handling of the chemicals was performed in a dry air glove box with a typical water content less than 10 ppm.

DOI: 10.1039/b103575b

The $M_2S_2O_7$–M_2SO_4(sat)–V_2O_5/SO_2(g) system

Mixtures of $M_2S_2O_7$ and M_2SO_4 were prepared by melting and mixing the components in a sealed ampoule. The solubility of sulfates in pyrosulfates is rather low,[11,12] *e.g.* the solubility of K_2SO_4 in $K_2S_2O_7$ is around 4 mole % at 450 °C. In order to ensure sulfate saturation even after a possible coordination of sulfate to V(IV), a mole fraction of sulfate, $X(M_2SO_4) \geqslant 0.06$ (of the binary system), was chosen, regardless of the alkali metal. Visual inspection of the molten samples confirmed excess sulfate as a white precipitate. V_2O_5 was added to this mixture at a M/V ($M_2S_2O_7/V_2O_5$) molar ratio of 40. The chemicals were filled into a quartz ampule (diameter = 12 mm, 300 mm length) in the glove box and sealed immediately under *ca.* 0.7 bar SO_2. The sealed ampules were transferred to a home made quartz tubular furnace wound with kanthal wire and were equilibrated for at least 100 h above the melting point of the mixture, *i.e.* 450–460 °C dependent on the type of alkali metal. From the furnace the ampules were dropped directly into icy water. Several attempts to quench into liquid nitrogen proved less successful, probably due to slow heat transfer through the N_2 gas film formed on the surface of the hot ampule. A too slow cooling of the samples resulted partly in formation of crystalline V(IV) compounds in the samples obscuring the EPR spectrum.

After quenching, the ampules were cut open in the glove box and some of the mixture ground and transferred to quartz capillary tubes (2.0 mm outer diameter, 0.5 mm wall thickness). The samples were sealed under vacuum. The capillary tubes were of unspecified quality, but tested negative for any EPR background signal (*e.g.* Fe(III)).

Samples with other M/V ratios were made by dilution of the M/V = 40 mixture with a premixed $M_2S_2O_7$–M_2SO_4 mixture.

The $M_2S_2O_7$–V_2O_5/SO_2(g) system

Samples without SO_4^{2-}-saturation are sensitive to the decomposition of the solvent melt, *i.e.* [eqn. (2)]

$$S_2O_7^{2-} \rightleftarrows SO_3 + SO_4^{2-} \quad (2)$$

which causes SO_4^{2-} contamination of the $M_2S_2O_7$. Only carefully selected batches of pyrosulfate of high purity were used. The mixing procedure was the same as in the previous case, except that the samples were not remelted and requenched after being transferred to the capillaries as in the case of the $M_2S_2O_7$–M_2SO_4(sat)–V_2O_5/SO_2(g) system. This was avoided in order not to decompose the pyrosulfate further. For the same reason no spectra of molten samples have been recorded. It was not possible to record well resolved spectra with M/V ratios smaller than 160, the spectra smeared out due to increased spin–spin relaxation.

Compound formation and isolation

The V(IV) compounds were synthesised in $M_2S_2O_7$–V_2O_5 melts with the alkali–vanadium ratios M/V = 3–5 in a pyrex flow cell and washed out with water (except for the mixed valence V(IV)–V(V) salt $K_6(VO)_4(SO_4)_8$ which is rather water soluble and prepared otherwise[14]) as described in detail earlier. The gas composition used was 10% SO_2, 11% O_2 and 79% N_2, corresponding to the synthesis gas in a traditional sulfuric acid plant. In the case of preparation of $K_6(VO)_4(SO_4)_8$, this gas was converted more than 90%, *i.e.* containing more than 9% SO_3.

EPR spectroscopy

The EPR spectra were recorded on a Bruker EMX spectrometer with a 12 kW 10″ magnet. Room temperature X-band spectra were recorded with a Bruker ER4102ST cavity. High temperature X-band spectra were recorded with a Bruker ER4114HT cavity whereas the room temperature Q-band spectra were obtained with a Bruker ER5106Q cavity.

Selected EPR spectra were simulated using the Simpow[15] computer program.

Spectrophotometric measurements

The optical spectrum was obtained using a Jasco 570 UV/VIS/NIR spectrophotometer. A sample of $M_2S_2O_7$–V_2O_5/SO_2(g) with M/V molar ratio of 40 was measured by placing the quartz capillary sample used for EPR measurements in the beam. Since a significant background signal was measured due to reflexions from the cylindrical quartz capillary tube the spectrum was fitted to a function with three gaussian terms and one constant (y_0) [eqn. (3)],

$$f(\nu) = y_0 + \sum_i \left(C_i \mathrm{e}^{\frac{-(\nu_i - \nu)^2}{2\sigma_i^2}} \right), \quad (3)$$

where C_i, ν_i, σ_i are the pre-exponential constant, the wave number of the peak and the line width parameter respectively for each peak, i, in the spectrum.

The spectrum was recorded in the range ν = 25000 cm^{-1} (400 nm) to 8000 cm^{-1} (1250 nm).

Results and discussion

The composition and structure of the V(IV) complexes in pyrosulfate melts are as mentioned not as well known as the V(V) complexes. Based on the knowledge of the V(V) complexes and a very recent investigation on V(IV) in pyrosulfate, the following reactions (4) and (5) will be considered for the rest of the discussion:

$$\text{Dissolution: } V_2O_5 + 2S_2O_7^{2-} \rightleftarrows (VO)_2O(SO_4)_4^{4-} \quad (4)$$

$$\text{Reduction: } (VO)_2O(SO_4)_4^{4-} + SO_2 \rightleftarrows 2VO(SO_4)_2^{2-} + SO_3 \quad (5)$$

Furthermore, in presence of excess sulfate the V(IV) complex will coordinate one additional sulfate [eqn. (6)]:

$$\text{Complex reaction: } VO(SO_4)_2^{2-} + SO_4^{2-} \rightleftarrows VO(SO_4)_3^{4-} \quad (6)$$

At the applied SO_2 pressure the equilibrium, eqn. (5), is almost completely shifted to the right, *i.e.* towards V(IV). A short V=O bond and four equatorial oxygen ligands from two bidentate sulfate ions are expected for $VO(SO_4)_2^{2-}$, since unidentate sulfate groups would lead to an unlikely coordination number of three instead of five where the *trans* position may coordinate additional sulfate (unidentately) to form the hexacoordinated $VO(SO_4)_3^{4-}$, which is coordinatively saturated. In $VO(SO_4)_2^{2-}$ the *trans* position will be free or loosely coordinated to the solvent. This type of coordination is common for the vanadyl(IV) cation.

The $M_2S_2O_7$–M_2SO_4(sat)–V_2O_5/SO_2(g) system

Fig. 1 shows the EPR spectra of samples with M/V = 40, 80 and 160 recorded in the X- and Q-band. All spectra are recorded at room temperature after quenching from 450–460 °C to 0 °C, except for the samples with M/V = 160 which in addition are recorded in the X-band in the molten state at 450–460 °C. The Q-band spectra of the samples with M/V = 160 have been simulated using the Simpow computer program.

The general EPR features of the quenched samples are quite similar with two general trends. The X- and Q-band spectra both show axial symmetry typical for octahedral VO^{2+} complexes with the hyperfine structure (due to coupling to the ^{51}V nucleus, I = 7/2), best resolved in the Q-band spectra. The line

Table 1 Spin Hamiltonian parameters, g and a (Gauss), of quenched and molten samples in the $M_2S_2O_7$–M_2SO_4(sat)–V_2O_5/SO_2 system

M	$g_\perp$	$g_\parallel$	$\Delta g_\parallel/\Delta g_\perp$ [a]	g_0 (450 °C)	g_0 (calc) [b]	$a_\perp$	$a_\parallel$	a_0 (450 °C)	a_0 (calc) [c]
Na	1.982	1.930	3.36	1.970	1.966	71.7	200	110	115
K	1.980	1.930	3.29	1.970	1.963	70.7	202	108	114
Rb	1.980	1.930	3.24	1.967	1.963	67.1	194	108	109
Cs	1.981	1.940	3.16	1.968	1.966	65.3	187	108	106

[a] $\Delta g_\parallel/\Delta g_\perp = g_e - g_\parallel/g_e - g_\perp$. [b] $g_0(\text{calc}) = 1/3(2g_\perp + g_\parallel)$. [c] $a_0(\text{calc}) = 1/3(2a_\perp + a_\parallel)$.

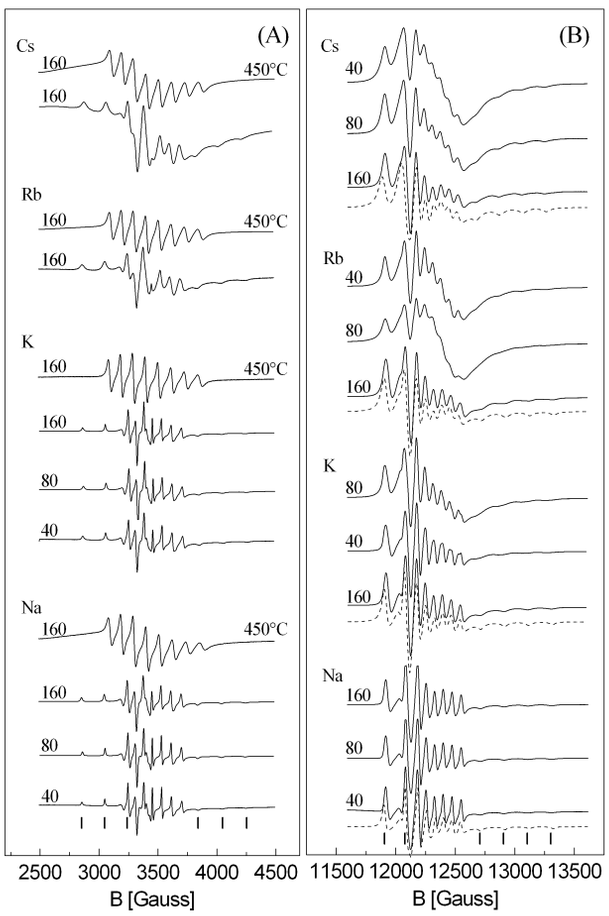

Fig. 1 X-band (A) and Q-band (B) EPR spectra of $VO(SO_4)_3^{4-}$ in the $M_2S_2O_7$–M_2SO_4(sat)–V_2O_5/SO_2(g) system with M/V = 40, 80 and 160 (M = Na, K, Rb and Cs). All spectra are recorded at room temperature after quenching from 450–460 °C except for the indicated M/V = 160 samples recorded at 450–460 °C in the X-band. Simulated spectra are shown stipulated.

width of the spectra increases with increasing vanadium concentration (lower M/V ratio) and with the molar weight of the alkali cation. The samples Rb/V = 40, Rb/V = 80, Cs/V = 40 and Cs/V = 80 could not be recorded with well resolved hyperfine structure in the X-band and are therefore not shown in Fig. 1.

The quenched spectra are typical immobilized axial symmetric spectra also known from, *e.g.*, frozen vanadyl-containing Schiff bases.[16,17] Axial symmetric spectra can be well characterized by g-tensors and hyperfine coupling constants, *i.e.* the parameters $g_\perp$, $g_\parallel$, $a_\perp$, $a_\parallel$ and one line width. The Q-band spectra, stipulated in Fig. 1, are computer simulations using these five parameters and assuming Lorentzian line shapes. The initial parameter sets for the iterations were obtained by an algorithm[16] using the well-resolved Q-band spectra. No differences were found in the parameters dependent on the vanadium concentration (within experimental error), hence the best resolved spectrum for each alkali metal was used for the accurate calculation of the EPR parameters, regardless of the concentration. The final parameters of the simulations are listed in Table 1. It can be seen that the parameters for the quenched samples are identical within the experimental error of ±0.005 and ±10 for g and a respectively, *i.e.* $g_\parallel = 1.930$, $g_\perp = 1.980$, $a_\parallel = 200$ Gauss, $a_\perp = 70$ Gauss. Only the parameters of the parallel feature for the Cs-based samples deviate slightly. It should be stressed that observable in-plane anisotropy rarely occurs in EPR spectra, even though some rhombicity is present.

However, the line width changes significantly by increasing size of the cation (Fig. 2). In order to discuss this, the line width

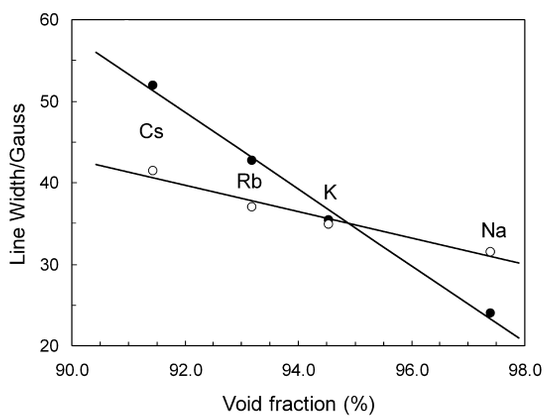

Fig. 2 Line width dependence on void fraction (see text) of the alkali metal cations M = Na, K, Rb, Cs in the $M_2S_2O_7$–M_2SO_4(sat)–V_2O_5/SO_2(g) system for samples with molar ratios M/V = 160 in the liquid state at 450 °C (open circles) and in the solid state at room temperature (filled circles).

for the M/V = 160 series has been plotted *versus* the void fraction (%), *i.e.* the volume fraction of the sample which is not occupied by the cation, $1 - (\frac{4}{3}N_A)V_m^{-1}\, r^3\, \pi$, r being the ionic radius of the cation, N_A Advogadro's number and V_m the molar volume of the sample. Since the samples are very dilute in vanadium, the molar volumes of the pure alkali pyrosulfates have been used.[18] The molar volume of the solid has been extrapolated from the liquid state. Fig. 2 shows this dependency both in the solid state at room temperature using the well resolved perpendicular components and in the molten state at 450–460 °C using the isotropic line width. Table 1 summarizes the parameters. Both in the solid and the liquid state an excellent linear correlation ($R^2 > 0.95$) is found, indicating that the line broadening can be explained solely by a spin–spin relaxation effect.

The high temperature X-band EPR spectra (Fig. 1A) of the molten samples with M/V = 160 exhibit eight isotropic lines of varying intensity as always found for monomeric vanadyl complexes in solution. The different alkali pyrosulfate solvents seem not to affect the first coordination sphere of the complex. Thus no variation in the isotropic g value or the isotropic hyperfine structure constant is observed as with respect to the type of the alkali cation. In some of the spectra, a skew baseline can be seen, probably due partly to formation of dimeric or polymeric V(IV) species where coupling along the chains may smear out the hyperfine structure. The measured isotropic parameters fit well with the calculated isotropic values from the quenched samples—considering the large temperature difference—as it can be seen in Table 1, indicating that we are dealing with the same complex in both phases.

Table 2 Spin Hamiltonian parameters, g and a (Gauss), of quenched samples in the $M_2S_2O_7$–V_2O_5/SO_2 system

M	$g_\perp$	$g_\parallel$	g_0 (calc)[a]	$\Delta g_\parallel/\Delta g_\perp$	$a_\perp$	$a_\parallel$	a_0 (calc)[a]
Na	1.978	1.912	1.956	3.714	81.6	210	124
K	1.977	1.912	1.955	3.567	81.7	211	125
Rb	1.976	1.917	1.956	3.242	79.9	206	122
Cs	1.978	1.918	1.958	3.467	78.4	204	120

[a] See Table 1.

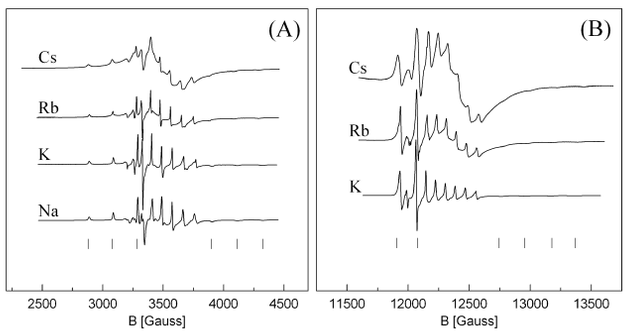

Fig. 3 X-band (A) and Q-band (B) EPR spectra of $VO(SO_4)_2^{2-}$ in the $M_2S_2O_7$–V_2O_5/SO_2(g) system with M/V = 160. All spectra are recorded at room temperature after quenching from 450–460 °C. Parallel features are indicated by "|" below the spectra.

The $M_2S_2O_7$–V_2O_5/SO_2 system

The X- and Q-band EPR spectra of the vanadyl complexes without sulfate saturation are shown in Fig. 3. The spectra represent axial symmetric complexes as in the sulfate saturated system, but the line width is much smaller, 5–15 G *vs.* 20–60 G for samples with sulfate saturation. This indicates that there is less distortion of the VO^{2+} unit for $VO(SO_4)_2^{2-}$ compared to $VO(SO_4)_3^{4-}$ complexes present in the sulfate saturated system. Furthermore, the EPR parameters of the parallel features are—not surprisingly—changed, as can be seen from Table 2. The value of $g_\parallel$ is typically about 0.015 smaller in the case of $VO(SO_4)_2^{2-}$ compared to $VO(SO_4)_3^{4-}$. The perpendicular components are less affected. This shows that the character of the V=O bond is important for the relaxation path of the unpaired electron.

This system seems to show the same trend on line width *versus* alkali metal as the sulfate saturated system, and even more pronounced. However it was not possible to record well resolved spectra of the Cs based system for proper determination of line widths, even at Cs/V = 160. An attempt to increase the Cs/V ratio further did not increase the resolution significantly, but decreased the S/N ratio unacceptably. The Rb based system suffered to some extent from the same problems. Furthermore it was impossible to expose the samples to high temperature without decomposition of the complex, and in the case of M = Na decomposition occurred already at room temperature which made it impossible to obtain pure spectra of Na/V = 160 in Q-band. Consequently, it was not possible to construct a line width *vs.* void fraction plot.

Properties of VO^{2+} compounds crystallized from pyrosulfate melts

The g-values for seven different compounds synthesized in our laboratories[19–21] have been determined by optimization using the Simpow program as shown in Table 3. The powder EPR spectra of several of the compounds have been given elsewhere. A varying degree of tetragonal distortion is found, judged from the g-anisotropy. These results show that EPR powder spectra of such compounds, which might appear isotropic from the immediate appearance of the spectra, actually exhibit anisotropy, which, however, becomes unresolved because of the relatively large line widths observed in these systems.

Electronic properties of VO^{2+} in pyrosulfate melts

According to the classic works[22,23] on the electronic assignment of VO^{2+} complexes, the $3d^1$ electron occupies the d_{xy} orbital in the ground state. Having a compressed octahedral geometry, the following simplified relations (7) and (8) between the paramagnetic and electronic transitions apply,[17,24,25]

$$\Delta g_\parallel = g_\parallel - g_e = -8\lambda\beta_1^{*2}\beta_2^{*2}/\Delta \quad (7)$$

$$\Delta g_\perp = g_\perp - g_e = -2\lambda\beta_2^{*2}\varepsilon_\pi^{*2}/\delta \quad (8)$$

λ being the spin–orbit coupling constant, where λ is estimated to be 170 cm^{-1} for the free V^{4+} ion, β_i^{*2} and ε_π^{*2} the wavefunction coefficients, $\Delta = E_{x^2-y^2} - E_{xy}$ and $\delta = E_{xz,yz} - E_{xy}$ are the energies for the electronic transitions between the indicated orbitals. The ratio $\Delta g_\parallel/\Delta g_\perp$ is very sensitive to tetragonal distortion—*e.g.* the strength of the vanadyl bond—of the octahedrons[26] since it is directly related to the energy ratio Δ/δ. From the data in Tables 1 and 2 it seems that the sulfate saturated vanadyl complexes are less distorted ($\Delta g_\parallel/\Delta g_\perp$ = 3.2–3.5) than the sulfate free complexes ($\Delta g_\parallel/\Delta g_\perp$ = 3.5–3.7), which shows that the *trans* coordinated sulfate in the saturated samples weakens the VO^{2+} bond, as expected. These complexes, however, are more distorted than VO^{2+} on oxide surfaces ($\Delta g_\parallel/\Delta g_\perp$ = 1–3), but less distorted than VO^{2+} in silicate glasses ($\Delta g_\parallel/\Delta g_\perp$ = 3–4.4).[27]

The value of β_2^{*2} can be obtained by equation (9):

$$\beta_2^{*2} = \frac{7}{6}\Delta g_\parallel - \frac{5}{12}\Delta g_\perp - \frac{7}{6}\frac{a_\parallel - a_\perp}{P} \quad (9)$$

where P is proportional to the expectation value of r^{-3} in the 3d orbitals of a free V^{4+} ion. A value of 184.5 Gauss is used in these calculations, as used by Sharma and co-workers.[26]

In Fig. 4, the optical spectrum of the complex present in the acidic quenched melt, $VO(SO_4)_2^{2-}$, is shown. The spectrum has

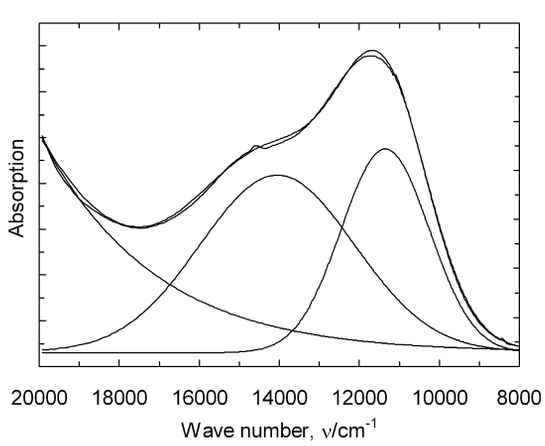

Fig. 4 Absorption spectrum of the vanadyl complex $VO(SO_4)_2^{2-}$ in the quenched $M_2S_2O_7$–V_2O_5/SO_2(g) system.

Table 3 EPR parameters for crystalline VO^{2+} compounds

Compound	$g_\perp$	$g_\parallel$	g_{iso} [a]	Ref.
β-$VOSO_4$	1.972	1.922		19
$Na_2VO(SO_4)_2$	1.970	1.939		20
$K_4(VO)_3(SO_4)_5$	1.962	1.969	1.964	21
$K_6(VO)_4(SO_4)_8$ [b]	1.978	1.930	1.972	14
$Rb_2(VO)_2(SO_4)_3$	1.977	1.917		[c]
$Cs_2(VO)_2(SO_4)_3$	1.977	1.913		[c]
$Na_{26}(VO)_5(SO_4)_{18}$	1.980	1.925		[c]

[a] Only where applicable. [b] Mixed valence V(IV)–V(V) compound. [c] Unpublished.

been resolved in three gaussian components as shown by resolved curves and a constant contribution for background correction. The summarized function (10) is

$$f(\nu) = 1.56 + 0.89\exp(-(\nu - 11350)^2/(2 \times 1100^2)) + 0.72\exp(-(\nu - 14050)^2/(2 \times 1930^2)) + 18500\exp(-(\nu - 77000)^2/(2 \times 12780^2)). \quad (10)$$

The last term has no physical/chemical meaning, but provides a mathematical fit of the absorption from the charge transfer and strong V(V) bands in the UV region.

The transition assigned as Δ in eqn. 7 corresponds to $d_{xy} \longrightarrow d_{x^2-y^2}$ and appears at 14050 cm^{-1} in $VO(SO_4)_2^{2-}$, while the transition assigned δ in eqn. (8) corresponds to $d_{xy} \longrightarrow d_{xz,yz}$, for the complex and is found at 11350 cm^{-1}. In the region above 20000 cm^{-1}, charge transfer bands well described[17,22,28] for VO^{2+} are seen, but contributions from traces of V(V) complexes in this region cannot be ruled out, since V(V) is known to absorb strongly in this region. Using the estimated value for λ of 170 cm^{-1} together with the observed energies for the d–d transition band from the optical spectra and the observed g- and A-values from the EPR measurements on the quenched melts, the wave function coefficients can be estimated for the complex $VO(SO_4)_2^{2-}$ in the frozen solution using eqns. (7)–(9).

This leads to the wave functions parameters, $\beta_1^{*2} = 1.028$, $\beta_2^{*2} = 0.907$ and $\varepsilon_\pi^{*2} = 0.894$. β_1^{*2} characterize the in-plane σ-bonding of $VO(SO_4)_2^{2-}$ and a value of one shows that there is no, or only very weak, covalent σ-bonding between the vanadium atom and the oxygen atoms in the equatorial ligand plane. The quantity $1 - \beta_2^{*2} = 0.093$ corresponds to the fraction of unpaired d electrons delocalised over ligand orbitals. This indicates a weaker V=O bond in this complex compared to $VO(H_2O)_5^{2+}$ and $VO(acac)_2$ but a possible effect from packing of the vanadyl units in the $Na_2S_2O_7$ structrure during quenching of the samples can't be ruled out. The term $(1 - \varepsilon_\pi^{*2}) = 0.106$ indicates some influence of π-bonding between vanadium and the vanadyl oxygen not unlike $VO(acac)_2$ which has chelating ligands such as $VO(SO_4)_2^{2-}$ is likely to have.

All wave function parameters, however, are close to unity compared to for example VO^{2+} on oxide surfaces. This indicates that the electronic properties of the vanadyl unit is well preserved even in this molten salt with high ionic strength of the solvent compared to aqueous solutions. This also gains support from the very similar molar absorptivity found to be around 19.0 l mol^{-1} cm^{-1} for VO^{2+} formed in both aqueous and pyrosulfate solvents.[2,27]

Conclusions

It has been shown that two VO^{2+} complexes exist in $M_2S_2O_7$–M_2SO_4–V_2O_5/SO_2(g) (M = Na, K, Rb or Cs) melts in the molar ratio range M/V = 40–160. The spin Hamiltonian parameters have been derived, and it has been shown that line broadening of the EPR spectra of these complexes due to spin–spin relaxation is evident. The electronic properties of VO^{2+} in pyrosulfate melts have been discussed by calculating wave function parameters, β_1^{*2}, β_2^{*2} and ε_π^{*2}, using the obtained spin Hamiltonian parameters and energy levels obtained from an absorption spectrum of $VO(SO_4)_2^{2-}$ in $Na_2S_2O_7$.

Acknowledgements

The authors wish to thank I. Laursen and K. Nielsen, Technical University of Denmark, for helpful discussions. NATO Science for Peace Programme (SfP 971984) has supported this investigation.

References

1 S. Boghosian, R. Fehrmann, N. J. Bjerrum and G. N. Papatheodorou, *J. Catal.*, 1989, **119**, 121.
2 D. A. Karydis, K. M. Eriksen, R. Fehrmann and S. Boghosian, *J. Chem. Soc., Dalton Trans.*, 1994, 2151.
3 O. B. Lapina, V. M. Mastikhin, A. A. Shubin, K. M. Eriksen and R. Fehrmann, *J. Mol. Catal.*, 1995, **99**, 123.
4 O. B. Lapina, V. V. Terskikh, A. A. Shubin, V. M. Mastikhin, K. M. Eriksen and R. Fehrmann, *J. Phys. Chem.*, 1997, **101**, 9188.
5 K. Nielsen, R. Fehrmann and K. M. Eriksen, *Inorg. Chem.*, 1993, **32**, 4825.
6 S. Boghosian, F. Borup and A. Chrissanthopoulos, *Catal. Lett.*, 1997, **48**, 145.
7 O. B. Lapina, B. S. Bal'zhinimaev, S. Boghosian, K. M. Eriksen and R. Fehrmann, *Catal. Today*, 1999, **51**, 469.
8 V. M. Mastikhin, G. M. Polyakova, Ya. Zyulkovskii and G. K. Boreskov, *Kinet. Katal*, 1970, **11**, 1463, *(Engl. Transl.*, 1971, **11**, 1219).
9 K. M. Eriksen, D. A. Karydis, S. Boghosian and R. Fehrmann, *J. Catal.*, 1995, **155**, 32.
10 K. M. Eriksen, R. Fehrmann and N. J. Bjerrum, *J. Catal*, 1991, **132**, 263.
11 S. B. Rasmussen, K. M. Eriksen and R. Fehrmann, *J. Phys. Chem*, 1999, **103**, 11282.
12 N. H. Hansen, R. Fehrmann and N. J. Bjerrum, *Inorg. Chem.*, 1982, **21**, 744.
13 G. E. Folkmann, G. Hatem, R. Fehrmann, M. Gaune-Escard and N. J. Bjerrum, *Inorg. Chem.*, 1991, **30**, 4057.
14 K. M. Eriksen, K. Nielsen and R. Fehrmann, *Inorg. Chem.*, 1996, **35**, 480.
15 M. Nilges, Program SIMPOW, Illinois ESR Research Center NIH, Illinois, IL, Division of Research Resources Grant No. RR0181.
16 N. D. Chasteen, in *Biological Magnetic Resonance*, ed. L. J. Berliner and J. Reubens, Plenum Press, New York, 1981, pp. 53; (please note misprints in formulas pp. 71–72).
17 D. Kivelson and S-K. Lee, *J. Chem. Phys.*, 1964, **41**, 1896.
18 G. Hatem, F. Abdoun, M. Gaune-Escard, K. M. Eriksen and R. Fehrmann, *Thermochim. Acta.*, 1998, **319**, 33.
19 S. Boghosian, K. M. Eriksen, R. Fehrmann and K. Nielsen, *Acta Chem. Scand.*, 1995, **49**, 703.
20 R. Fehrmann, S. Boghosian, G. N. Papatheodorou, K. Nielsen and R. W. Berg, *Inorg. Chem.*, 1991, **29**, 3294.
21 R. Fehrmann, S. Boghosian, G. N. Papathedorou, K. Nielsen and R. W. Berg, *Inorg. Chem.*, 1989, **28**, 1847.
22 C. J. Ballhausen and H. B. Gray, *Inorg. Chem.*, 1962, **1**, 111.
23 C. K. Jørgensen, *Acta Chem. Scand.*, 1957, **11**, 73.
24 N. M. Atherton, in *Principles of Electron Magnetic Resonance*, ed. T. J. Kemp, Ellis Horwood, Chichester, 1993.
25 K. Dyrek and M. Che, *Chem. Rev.*, 1997, **97**, 305.
26 V. K. Sharma, A. Wokaun and A. Baiker, *J. Phys. Chem.*, 1986, **90**, 2715.
27 H. Farah, M. P. Brungs, D. J. Miller and G. R. Belton, *Phys. Chem. Glasses*, 1998, **39**, 318.
28 J. Selbin, *Coord. Chem. Rev.*, 1966, **1**, 293.